1. OVERVIEW OF THE HIPPARCOS SATELLITE

This chapter describes the operating principle of the Hipparcos satellite, with reference to the measurement principle, the constraints and properties of the nominal satellite orbit, and the satellite environmental conditions. An overview of the main satellite subsystems: attitude control, data handling and on-board processing, the mechanical and electrical design, and the overall operational concept—is given, along with a description of the ground segment. The scientific and operational concepts introduced in this chapter are described in greater detail in subsequent chapters.

1.1. Operating Principle

The primary goal of the Hipparcos mission was the measurement of the positions, proper motions, and trigonometric parallaxes of about 120 000 stars. To achieve this, a special optical telescope was designed to function on a spacecraft placed in geostationary orbit, above the Earth's atmosphere. The telescope had two fields of view, each of size $0\overset{\circ}{.}9 \times 0\overset{\circ}{.}9$, and separated by about 58°. The satellite was designed to spin slowly, completing a full revolution about its spin axis in just over two hours. At the same time, it could be controlled so that there was a slow change in the direction of the axis of rotation. In this way, the telescope could scan the complete celestial sphere.

Measurements of the angles between pairs of stars, inferred from the relative phases of the modulated signals created by the main grid, were built up over the three-year lifetime of the satellite in orbit. From many such measurements, made at many different orientations, and at many different epochs, a whole-sky astrometric catalogue (the Hipparcos Catalogue) was built up, containing the positions, parallaxes, and proper motions of all of the stars on the pre-defined observing list. This list, which contained about 120 000 stars, constituted the so-called 'Hipparcos Input Catalogue'. The Tycho Catalogue was constructed from the data sent to the ground from the satellite's star mapper.

The measurement principle of Hipparcos is illustrated in Figure 1.1. The payload was centred around an all-reflective Schmidt telescope with an entrance pupil of 290 mm and a focal length of 1400 mm, the light from two sections or 'fields' of the sky was conveyed through two baffles, set at a fixed angle of close to 58°. A 'beam combiner' allowed the

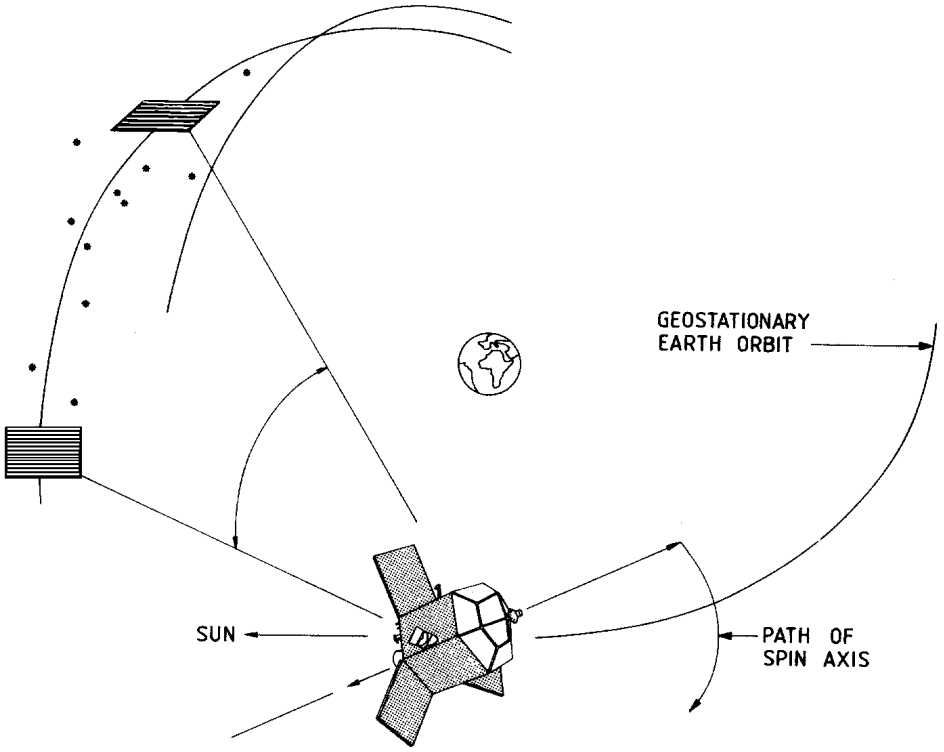

Figure 1.1. *The measurement principle of the Hipparcos satellite. The two fields of view scanned the sky continuously, and relative positions of the stars along the scanning direction were determined from the modulated signals resulting from the satellite motion. Although the nominal geostationary orbit was not achieved, the same scanning motion was implemented in the actual (transfer) orbit.*

two fields to be projected onto the same focal surface by means of the spherical primary mirror. It was then possible to determine the true angle between two stars, one in each field of view, by using the known or 'basic angle' of 58° between the two fields of view, plus the apparent separation measured on the focal surface of the telescope. This choice for the basic angle was influenced by the goal of connecting stars with very different parallax factors by measurements within the combined field of view. The precise value chosen was selected by considering the 'rigidity' of the resulting measurements made over a great circle scanned by the satellite, as illustrated in Figure 1.2.

As the satellite slowly rotated at its nominal scanning velocity of approximately 1 revolution every 2 hours 8 minutes, the images of the stars in the fields of view moved across the focal plane grids. These signals were sampled by detectors behind these grids. Two different types of detector were used in the Hipparcos payload—an image dissector tube for the main grid and photomultiplier tubes for the star mapper grids. To protect the detectors from excessive illumination due to occultations by the Earth and Moon, shutters were built into the payload so that the detector photocathodes could be shielded from the bright occulting source.

The surface on which the two fields of view were focused contained 2688 parallel slits in an area of about 2.5×2.5 cm^2, covering about $0\overset{\circ}{.}9 \times 0\overset{\circ}{.}9$ on the sky (see Figure 2.10). As the telescope slowly scanned the sky, the star light was modulated by the slit system, and the modulated light was sampled by an image dissector tube

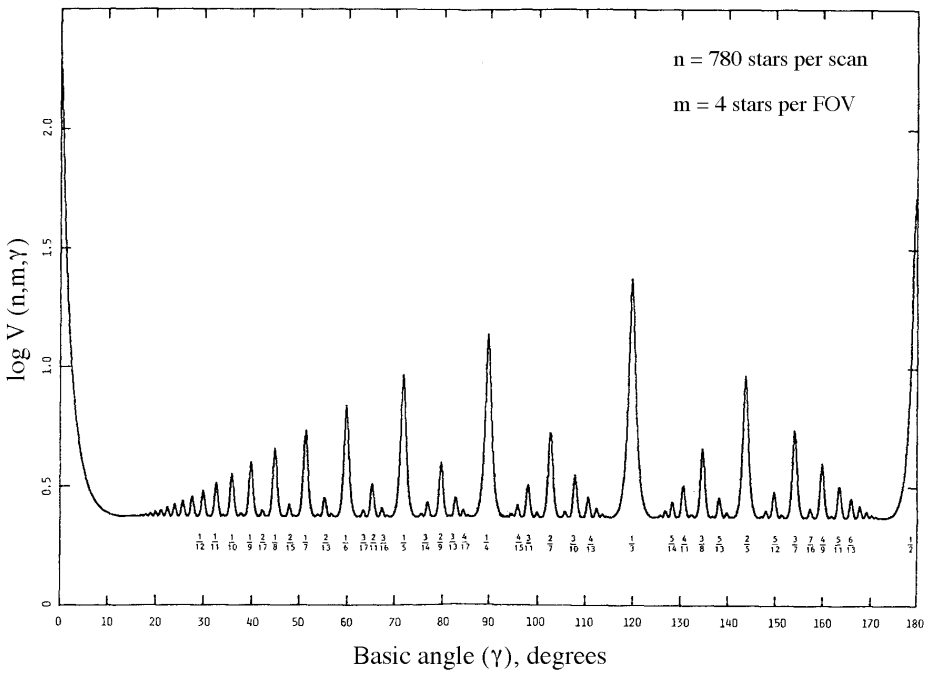

Figure 1.2. *The 'rigidity' of the solution for star abscissae on a great circle scanned by the satellite is strongly influenced by the choice of the 'basic angle' between the two fields of view. The chosen value of 58° was selected as providing good rigidity (resulting from good connectivity between the stars observed on each great circle), at the same time allowing the simultaneous measurements of stars having very different parallax factors. Peaks in the function indicate basic angles which would be unsuitable from the point of view of the rigidity of the great circle solutions. FOV refers to field of view.*

detector, at a frequency of 1200 Hz. At any one time, some four or five of the selected (or programme) stars were present in the two fields of view. The image dissector tube consisted of a photomultiplier with an electromagnetic deflection system that allowed only one small part of the photocathode to be sampled at any given time. This small sensitive area, referred to as the instantaneous field of view, covered an area of about 38 arcsec in diameter (projected on the sky). The size of the instantaneous field of view was minimised as the result of a 'piloting budget', accounting for the *a priori* errors on the star positions, the performance of the satellite real-time attitude determination, and the fact that the instantaneous field of view was stepped discretely to follow the moving star images.

The detector could only follow the path of one star at a time, but under rapid computer control it was able to track all the programme stars for short intervals of time during their passage across the field, which took about 20 s. In this way, measurements of the relative positions of the programme stars were continually being made, distributing the available observing time amongst the visible stars, the observations being made quasi-simultaneously in order to eliminate any residual attitude jitter. Due to the scanning motion of the satellite, the majority of stars in the field of view at any time appeared first in the preceding field of view, and then in the following field of view about 20 minutes later. As the scans also overlapped laterally when the satellite rotation axis changed on each sweep of the sky, the stars would appear again, but this time compared with other stars. In this way, a dense net of one-dimensional measurements of the relative separations of the stars was slowly built up.

The satellite spin axis was kept at a constant inclination of approximately 43° to the direction of the Sun, and revolved around the Sun once in approximately eight weeks, resulting in a continuous and systematic scanning of the celestial sphere. Throughout the scanning motion the satellite therefore remained in a constant thermal environment, modulated only by the satellite rotation. Any region of the sky was scanned many times during the mission by great circles which intersected at well-inclined angles as a result of the choice of the 43° sun aspect angle. A typical star was observed some 80 times in each field of view throughout the lifetime of the satellite. The number of possible connections between the observed stars was considerably enhanced due to the almost simultaneous observation of stars separated by the large basic angle. The individual measurements were combined to form the final Hipparcos Catalogue, including the displacements due to parallax and proper motion, using techniques similar to those used in triangulation in surveying the Earth's surface.

The real-time attitude determination on board, required for autonomous piloting of the detector's instantaneous field of view, was achieved by the on-board computer using the spacecraft rotation rates, as measured by three independent gyros, the biases in those gyros (the gyro drifts), knowledge of times and durations of thruster firings, and critically, the measurements of transit times of stars crossing the star mapper grid. By comparing the measured crossing times of designated stars with those expected from the theoretical motion of the spacecraft, it was possible for the on-board computer, using a Kalman filter, to estimate the amount that the spacecraft had deviated from the predefined attitude.

The image dissector tube signal, as modulated by the main grid, was assumed to be of the form (see Figure 1.3):

$$I(t) = I_{BG} + I_0[1 + M_1 \cos(2\pi\omega t + \theta_1) + M_2 \cos(4\pi\omega t + \theta_2)] \qquad [1.1]$$

where:

- $I(t)$ is the instantaneous count rate at time t
- I_{BG} is an additional signal due to background noise and detector dark current
- I_0 is the mean count rate for the observed star (dependent on magnitude and colour)
- M_1 is the first modulation coefficient for the observed star
- M_2 is the second modulation coefficient for the observed star
- t is the time relative to a reference observation (mid-frame) time (s)
- ω is the grid frequency of the image dissector tube signal in Hz, i.e. $\omega = v/s$ where v is the angular scanning velocity of the satellite (arcsec s^{-1}), and s is the grid slit spacing (arcsec)
- θ_1 is the phase of the first harmonic of the signal at $t = 0$
- θ_2 is the phase of the second harmonic of the signal at $t = 0$

In addition to the main instrument (there was a second image dissector tube detector provided for redundancy), the payload included two star mappers, the second also being provided for redundancy purposes—the non-operational detectors were usually switched off when not in use. The function of the star mapper was to provide data allowing real-time satellite attitude determination, a task performed on-board the satellite, as well as the *a posteriori* reconstruction of the attitude, a task carried out on the ground. The continuous flow of star mapper data was also used to create the Tycho Catalogue,

comprising astrometric and two-colour photometric measurements of all stars, down to about 10–11 mag.

The star mapper consisted of a star mapper grid, located at opposite sides of the primary modulating grid (see Figure 2.10), and two photomultipliers measuring the light transmitted by the whole star mapper grid in two different spectral bands, roughly corresponding to the Johnson B (blue) and V (visual) bands. The spectral separation was performed by means of a dichroic beam splitter, which directed that part of the signal with $\lambda < 465$ nm toward the 'blue' photomultiplier (referred to as the B_T channel) and that part of the signal with $\lambda > 475$ nm toward the 'visible' photomultiplier (the V_T channel)—the subscripts 'T' referring to Tycho, and drawing attention to the distinction between the Tycho and Johnson photometric systems.

Each star mapper consisted of two sets of four slits, each set at different inclinations with respect to the scanning direction, so that the satellite attitude could be derived from the photomultiplier signals as the star images moved across the grid. Both channels were sampled at 600 Hz by the on-board data handling subsystem. In total, the image dissector tube and star mapper data comprised 83 per cent of the telemetry stream.

The photomultiplier tube signal for each of the star mapper channels was assumed to be of the form (see Figure 1.4):

$$I^*(t) = I^*_{BG} + I^*_0 \sum_{k=1}^{N} S(vt - p_k) \qquad [1.2]$$

where:

$I^*(t)$ is the instantaneous count rate at time t

I^*_{BG} is an additional signal due to background noise and detector dark current

I^*_0 is the peak count rate at the centre of a slit

N is the number of slits in a slit system ($N = 4$)

$S(x)$ is the single-slit response function, i.e. the normalised signal transmission factor as a function of distance from the source to the centre of the slit, in arcsec

v is the angular scanning velocity of the satellite (arcsec s^{-1})

t is the time relative to the central observation time (s)

p_k is the position of the k-th slit in the slit system (arcsec)

The payload is described in detail in Chapters 2 and 3. The nominal scanning law and the star observing strategy are described in Chapter 8. The processing of the main grid and star mapper data, leading to the construction of the Hipparcos and Tycho Catalogues, are described in detail in Volumes 3 and 4 respectively.

The spacecraft provided the structure platform for mounting the payload main assembly via an interface structure, the external baffles to protect the detectors from stray light from the Sun and the Earth, and the appropriate mounting surfaces for all spacecraft hardware including the apogee boost motor, solar arrays and antennae. In addition, the spacecraft supported a shade structure surrounding the payload which ensured maximum thermal decoupling from the external environment.

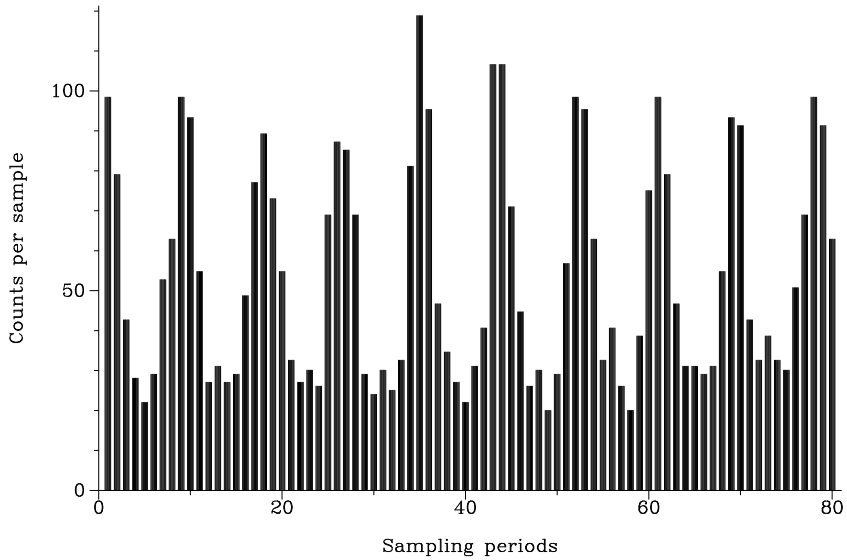

Figure 1.3. *Image dissector tube signal. The information transmitted to the ground from the main detector consisted of the photon counts per 1200 Hz sample. The main peaks correspond to the first signal harmonic, and the (marginally visible) intermediate peaks correspond to the second harmonic. The brightness of the star at the time of the measurement is given by the amplitude of the signal, while the phase of the modulated signal with respect to some reference phase provides the relative position of the star image, along the scanning direction, modulo one grid step. The data corresponds to observations of 1/15 s for HIP 114347, Hp = 5.3 mag, in April 1991.*

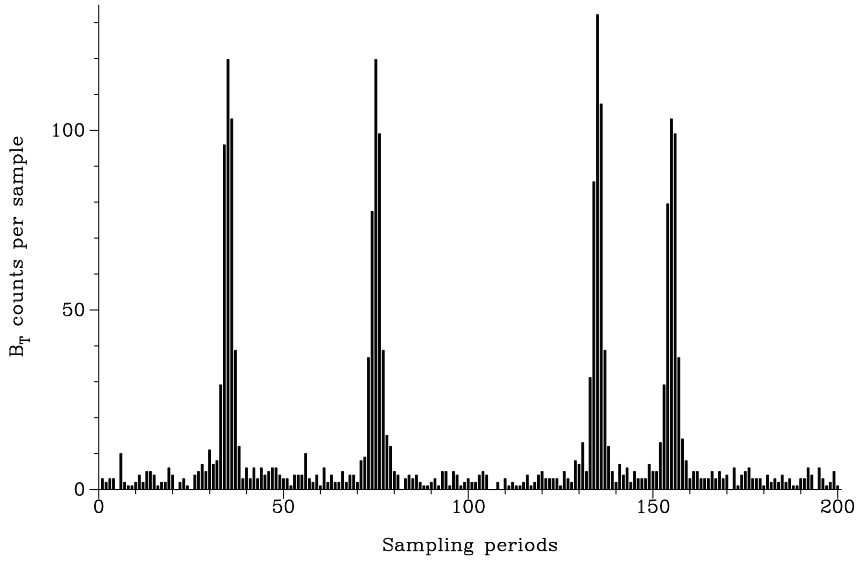

Figure 1.4. *Photomultiplier tube signal (blue channel) for the transit of one star over a single slit system. The information transmitted to the ground from the star mapper detector consisted of the photon counts per 600 Hz sample measured simultaneously in the B_T and V_T channels. The four peaks corresponding to the four aperiodically spaced star mapper slits, yield the star intensity and position after appropriate filtering. The observation is for HIP 35946, B_T = 6.62 mag, transits for the vertical slits and the following field of view.*

1.2. Constraints and Properties of the Nominal Orbit

Due to the measurement principle of Hipparcos, which needed as input a continuously updated 'programme star file' of star positions predicted to cross the instrument's field of view as a function of time, the satellite required permanent attendance by the ground segment in order to pursue the nominal mission. This requirement would have been best fulfilled by a geostationary orbit (equatorial plane, 36 000 km height, 24-hour period), which would have kept the satellite in a fixed position with respect to a single ground station. From this orbit, as opposed to low-Earth orbits, the Earth obscures only a small portion of the celestial sphere being scanned. The station 12°W was originally chosen from the geostationary orbit segments available in order to optimise the accuracy of the orbit determination from the single ground station. In practice, the target geostationary orbit was not achieved, and the mission was conducted with the satellite in a highly elliptic geostationary transfer orbit, as described more fully in subsequent chapters.

Eclipse Operations

For a period of 45 days around the two equinoxes, the orientation of the nominal Hipparcos (geostationary) orbit relative to the ecliptic was such that the Earth would have passed between the Sun and the satellite every 24 hours. Such eclipses would have lasted up to 72 minutes, during which time there would be no energy input to the solar arrays and the power subsystem would have to rely on its batteries. At the same time, the heat input would fall, changing the thermal balance of the satellite. While the satellite had been designed for these eclipse conditions, extreme eclipse durations were considerably longer for the actual geostationary transfer orbit, placing complex constraints on the power subsystem at these times.

Occultation of the Fields of View

The satellite scanned the sky with its spin axis pointed in a direction that moved only slowly, with an orbital period in its actual geostationary transfer orbit of 10.66 hours. This meant that the scanning great circle intercepted the Earth's disc about four times per day, with all or part of each field of view being exposed to this bright source in one or more consecutive scans. Since the Earth is very bright from such an orbit, shutters in front of the detectors were closed some time before the actual disc of the Earth entered the field of view, and they remained closed until after it had passed. The actual duration of the interruption was determined by the straylight protection characteristics of the payload baffles, and ranged from a few minutes to more than one hour. Similar interruptions were caused by occultation due to the Moon although, subtending a smaller angle and being less bright, the corresponding interruptions were shorter.

The impacts of such interruptions in data collection were threefold: (i) the 'dead time' had to be accounted for in estimating the mission duration needed for the required number of scientific measurements; (ii) the rigidity of solution of the great-circle equations would be degraded if measurements could not be linked between the two fields of view and between consecutive revolutions; and (iii) while the star mapper was not

operating the satellite attitude would drift with only gyroscope measurements, leading to degradation in pointing accuracy and even additional operations needed to return to the nominal scanning law after the interruption.

Simulations showed that the dead time for the nominal geostationary orbit, due to occultations, would be about 5 per cent, which was within the budget foreseen during mission definition, and that mission accuracy requirements could be achieved with up to 40 per cent of great circles interrupted, which exceeded the predicted percentage for the nominal geostationary orbit with a clear margin. The real-time attitude determination performance was also demonstrated in simulations, showing that conditions leading to the need for a full reinitialisation of the pointing would occur only once or twice in the entire mission. In practice, as a consequence of the revised orbit, dead time was significantly larger, and pointing reinitialisation was frequently required.

1.3. Satellite Environmental Conditions

The following environment conditions expected for the nominal geostationary orbit were taken into account in the overall satellite design.

Mechanical Environment

The dominant mechanical environment driving the satellite design was that encountered during the launch phase, which exposed the satellite to static and quasi-static accelerations, random vibration, and acoustic sound pressure.

Thermal Environment

There were two cases of thermal environment driving the design: (a) the transfer and near synchronous orbit, when the satellite was spinning, the solar arrays were stowed, the internal power consumption was low, and the sun aspect angle with respect to the spin axis was between 90° and 115° (the upper limit of the sun aspect angle determined by the launch window); and (b) the geosynchronous orbit, when the satellite would be three-axes controlled, the solar arrays would be deployed, the internal power consumption would be high, and the sun aspect angle would be 43°.

The sun aspect angle was given by the nominal scanning law, but could go to 0° ('sun-pointing') for emergency sun acquisition and for initialisation. The thermal design had to cope with both somewhat contradictory cases by appropriate multi-layer insulation, radiators, and electrical heaters. The compliance of the satellite with the thermal environment, in addition to comprehensive mathematical modelling and analyses, was verified by thermal-balance and the thermal-vacuum tests before launch.

Electromagnetic Environment

The electromagnetic environment was generated externally by the launch vehicle and the passenger satellite in the dual launch, and internally by the satellite electrical equipment. A margin between electromagnetic emission and electromagnetic susceptibility

was ensured by introducing a strict grounding and isolation scheme, careful shielding of units and harness, and interface circuits with common mode rejection capability.

Radiation Environment

Semiconductor lifetime: Semiconductors degrade when exposed to ionising radiation. The degradation of high-reliability component parameters as a function of radiation dose is well known, and this degradation had to be taken into account as a life-limiting factor. For each electronic unit, a radiation analysis was performed, consisting of computing the dose a component would be subjected to, taking into account the radiation shielding of the surrounding material of the unit and the satellite. Then, either the circuit design was able to accommodate the degraded parameters at the projected end of life, or additional local shielding had to be applied.

Single event upset: The 'single event upset' effect is the result of a high-density ionisation due to heavy and high-energy particles. It can cause such a high local charge deposition in a semiconductor that the logical state of a flop-flip or a memory cell is changed. Although this is generally a recoverable error, and no permanent damage results, it can upset the on-board computer systems. The satellite system was designed in such a way that no computer function was crucial for the satellite safety. However, a frequent computer upset would interrupt and degrade the mission.

The following measures were taken to protect the satellite against single event upsets: (a) the control law electronics used a processor of low radiation susceptibility, while the control law electronics memory employed an 'error detection and correction logic' which corrected any single bit error; and (b) the on-board computer used a radiation-hardened processor. The on-board computer memory was continuously checked for parity errors, which then had to be corrected from ground.

Electrostatic discharge: Electrostatic discharges have troubled many geostationary satellites. In a plasma environment, the satellite surfaces are charged up to different potentials, depending on the material properties and sun illumination. The potential differences can reach a few thousand volts, sufficient to cause sudden electrostatic discharges which interfere with the satellite electrical system. Hipparcos was designed to avoid differential charge-up, and also to provide protection against discharge effects should they occur.

To avoid differential charge-up, all surfaces exposed to space were required to be electrically conductive. This requirement had a significant impact on the thermal control design, as it ruled out the most conventional thermal control materials. The surface materials selected for the satellite were conductive black paint, aluminium and indium-tin-oxide coated optical surface reflectors. The only compromise, made for cost reasons, was the non-conductive glass cover of the solar cells. To verify that no differential charge-up could occur, mathematical models to analyse the phenomenon of electrostatic discharge were performed. The properties of the satellite surface materials, which were a sensitive input to the analyses, were measured in a special test programme performed within the development programme.

To protect against discharge effects, the whole spacecraft was shielded. This was done implicitly in the lower part of the spacecraft by aluminium panels forming a metallic box to house the spacecraft equipment. The upper part was mainly framework, supporting

the multi-layer insulation to protect the payload. A 0.1 mm thick aluminium foil surrounding the framework formed the electrostatic discharge shield.

Electrostatic discharge protection was also the driver for the electrical grounding and isolation concept. The concept chosen was a distributed single-point grounding scheme. Each box had its own secondary power supply, isolated from the main bus and grounded to the box structure, thus providing the box signal ground. Signal lines between boxes had common-mode rejection capability—signal receivers were either differential amplifiers, opto-couplers, or floating relay coils. For digital links, standardised transmitters and receivers were developed for use by all electrical subsystems, referred to as the 'standard balanced digital link'.

Darkening of optical elements: Prolonged exposure to ionising radiation can alter the transmission characteristics of optical materials. The extent of transmission loss is wavelength-dependent, being more significant for shorter wavelengths. During its operation, the satellite would be continuously exposed to trapped electrons and protons in the Earth's outer radiation belts. Although the protons would not normally be sufficiently energetic to penetrate the outer wall of the satellite, any so-called 'anomalously large solar events' could generate increased levels of high-energy protons.

In order to minimise the effects of this radiation, the transmitting optical elements were made of glass types that showed maximum resistance to irradiation darkening, subject to their general properties (spectral transmission and refractive index) being compatible with the requirements of the mission. At the same time, the relay optics and detector windows were shielded by layers of aluminium, and additional material was added to the structural elements to provide shielding in directions where this was not already provided by existing hardware.

In assessing the predicted end-of-mission performance in advance of launch, the expected degradation of optical transmission was calculated on the basis of the best-available knowledge of the radiation environment in geostationary orbit, and accounting for two anomalously large solar flares. This was considered to be consistent with previous experience at the phase of the solar cycle (around maximum) at which the Hipparcos measurements would take place.

The Cerenkov effect: A charged particle passing through a transparent dielectric medium with a velocity greater than the velocity of light in the medium, emits visible electromagnetic (Cerenkov) radiation. The Earth's outer radiation belts, through which the (nominal and actual) orbit of Hipparcos passed, contained electrons sufficiently energetic to generate light by this effect in the dioptric elements of the payload optics.

Depending on the direction of motion of the individual electron and the distance of each optical element from the detector, the part of the emitted light that falls within the spectral measurement range may make a significant contribution to the background count rate, against which the stellar signals had to be detected and measured. However, the pulse width of the Cerenkov light flash being much smaller (~ 0.1 ns) than the time resolution of the photomultiplier (~ 40 ns), one or more photons generated by each incident high-energy electron would produce just one pulse recognised above the discriminator threshold as a background count.

The measures implemented to counteract this effect included the provision of additional material to shield sensitive elements in directions where such shielding was not provided

by the satellite hardware itself, and the masking of unused areas of transmitting optics. The radiation shielding requirements were estimated by Monte-Carlo studies.

It was verified that the predicted residual count rate would not induce an unacceptable degradation of mission performance. The effect was particularly important for the star mapper, because of its large field of view, where it was expected to contribute the major part of the background count rate. For the main mission, the use of a restricted instantaneous field of view was expected to reduce drastically the proportion of the emitted light to which the detector was sensitive.

1.4. Attitude Control Concept

The attitude and orbit control subsystem provided the control, stabilisation and measurement about the three satellite axes during all phases of the mission, and performed all orbit manoeuvres. Orbit reconstitution data with an accuracy of about 1.5 km in the instantaneous satellite position and 0.2 m s^{-1} in the instantaneous velocity vector were performed at ESOC. The attitude determination used rate-integrating gyroscopes, the drifts of which were calibrated in real-time using star mapper data from star crossings occurring every 20 s on average, although later in the mission, as a result of progressive gyro failures, the gyro input had to be replaced by star mapper data and a disturbance-torque model. Cold nitrogen thrusters (with a nominal thrust of 0.02 N) were used for the attitude control.

An extremely smooth satellite motion was required because of the measurement principle. The sequential detection of the grid-modulated light from each star made the phase extraction sensitive to any jitter during this sequence. Furthermore, the interlacing of bright and well-measured stars along a great circle depended on the smoothness and predictability of the motion. This interlacing significantly improved the astrometric accuracy. Therefore, the trade-off and selection of the attitude control concept was one of the key decisions influencing the feasibility and performance of the Hipparcos mission. The decision was complicated by the difficulty of acquiring experimental data on microvibration in a 1*g* environment, and by doubts about the applicability of conventional finite-element models to this problem. The attitude control candidates considered during the early phases of the satellite design were reaction wheels, magnetic actuators and small thrusters:

(i) reaction wheels, the classical means of providing a continuous attitude control, were discarded, because of the resulting high level of attitude jitter caused by bearing noise. This problem could not be solved by considering the use of mini reaction wheels, or reaction wheels with magnetic bearings, or special suspension mounts for the wheels;

(ii) magnetic torquers, i.e. magnetic coils generating a torque within the Earth's magnetic field, were discarded, because there are uncontrollable areas depending on the angle between the coil and the Earth's magnetic field, which would still require additional reaction wheels. The control is complex, and depends on the attitude to the Earth's magnetic field, which would vary throughout the mission as a consequence of the adopted scanning law. Also, the Earth's magnetic field itself can vary significantly during magnetic storms. Furthermore, the magnetic actuators could interfere with the image dissector tube detector, which was inherently magnetically sensitive;

(iii) small thrusters, when actuated, cause an attitude discontinuity and excite an attitude jitter. This was shown to be acceptable if the actuations were not too frequent, sufficiently weak and with higher frequencies suppressed, and if the jitter could be damped out to acceptable levels in a time period small compared with the time for which a star would be observed.

The last of these attitude-control concepts was chosen, with specially designed 0.02 N 'cold gas' thrusters. The satellite was designed to operate in free drift in a ±10 arcmin band around the orientation given by the nominal scanning law. If any axis exceeded this band, the thrusters would be fired. If, at the same time, the other axes exceeded a narrower inner band, their thrusters would also be fired in a synchronised manner. This synchronised firing scheme, plus an optimisation of impulse bit and disturbance torque prediction, led to a predicted average time between thruster firings of 400 s, with the firings causing a disturbance for less than 2 s.

Other sources of jitter that had been carefully assessed before launch, in addition to that due to gas jet actuations, were gyro mechanical noise, apogee boost motor residuals, payload shutter mechanism actuations, and the impact effects of micrometeorites. In addition, the frequencies to which the measurement principle and the star observing strategy were especially sensitive were avoided by suitable control of the satellite natural frequencies.

1.5. Data Handling and Processing

The system design for the on-board data handling and data processing was determined by the following requirements:

(a) the continuous uplink of *a priori* star position and magnitude information from the Hipparcos Input Catalogue in the form of the programme star file, for a look-ahead time of several minutes;

(b) the real-time computation of the star observing strategy and the image dissector tube piloting from the programme star file and the actual satellite attitude;

(c) the real-time attitude determination from gyro and star mapper data with a high degree of accuracy (1 arcsec) as an input to the star observing strategy and image dissector tube piloting;

(d) the time tagging of the measurements with a stability of 5 μs over 5 minutes, corresponding to a satellite spin phase of about 1 milliarcsec (5 minutes roughly corresponded to the time between bright, well-measured stars to be linked on a great circle).

As a result of this architecture, the on-board processing was shared between two computers: the central on-board processor and the control-law electronics. The on-board computer performed the star observing strategy and the detector piloting. In addition, it performed the 'outer loop' of the real-time attitude determination, based on reference star data from the programme star file, and on measurements from the star mapper. It also performed the thermal control of the payload. The control-law electronics performed the 'inner loop' of the real-time attitude determination, based on gyro data, and also the control law which generated the commands for the thrusters.

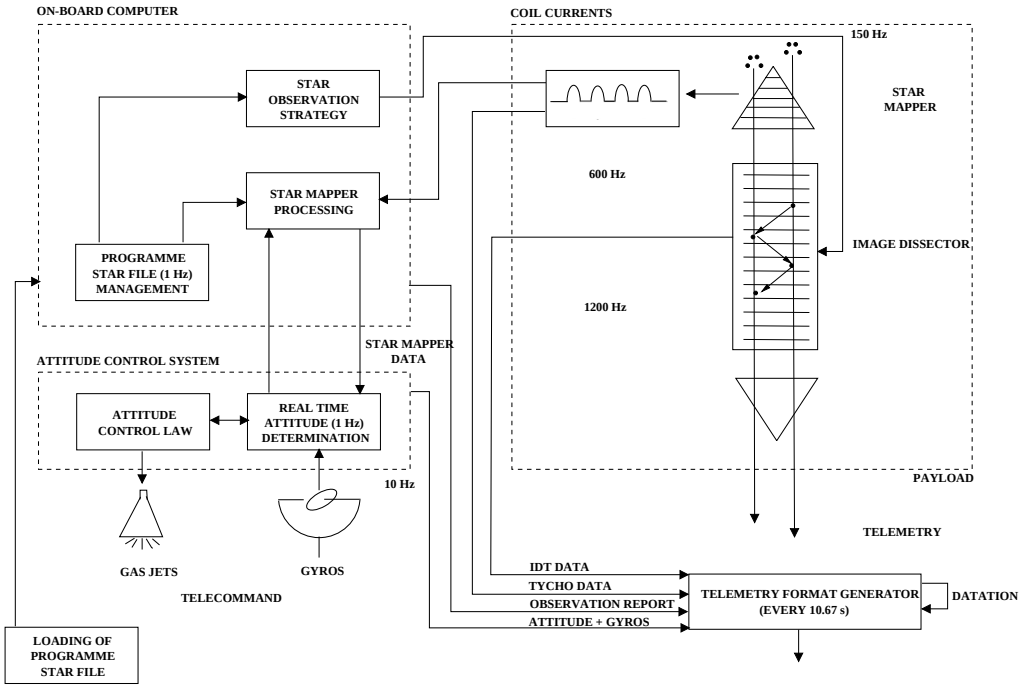

Figure 1.5. *A block diagram of the main measurement and operational functions on board the satellite. To the top left, the uplinked programme star file was used by the on-board computer to determine the details of the star observing strategy over the coming minutes. Information on the satellite attitude was provided by a combination of gyro and star mapper data (bottom left), which was also used to determine the gas jet actuations necessary to maintain the satellite in its pre-defined scanning law. Attitude information and information from the programme star file was used to point the instantaneous field of view of the image dissector tube, and to acquire relevant extracts of the star mapper data stream (top right). All relevant data were interleaved and sent to ground in real time (bottom right).*

The whole on-board system was synchronised by broadcast pulses. The piloting, the image dissector tube sampling, and the format generation was synchronised in 150 Hz cycles. Thus, the time tagging of the payload data was given implictly by the location within the telemetry format. The less time-critical on-board computer and control-law electronics data were interleaved into fixed telemetry format slots as packet telemetry. The on-board computer and control-law electronics computations were synchronised by the telemetry format pulse.

The overall concept of the acquisition of scientific data by the satellite is depicted in Figure 1.5. The programme star file was loaded from ground. It contained information on the programme stars to be observed by the image dissector tube, and reference stars used to perform the attitude determination on-board. The programme star file was managed by the central on-board software.

The central on-board software retrieved information about the reference stars from the programme star file and, by means of attitude information from the attitude and orbit control system, computed the expected transit time of the reference stars passing over the star mapper slits. In a time window around the expected transit time, star mapper samples were acquired and filtered to determine the actual transit time of the reference star. The difference between expected and measured transits was then used as an error signal for the attitude determination, which was continuously performed for the three axes by means of gyro measurements. The real-time attitude determination

outputs were used for attitude control within a band of ±10 arcmin around the nominal scanning law, and for computing the positions of programme stars in the field of view for proper piloting of the image dissector tube.

The central on-board software retrieved information about the programme stars that were to appear in the field of view for the next observation frame of $T_4 = 2.133\ldots$ s and computed the star observing strategy, i.e. the pattern of interleaved subsequent star observations, according to star criteria contained in the programme star file. These criteria were priority, target observation time, and minimum observation time (see Chapter 8 for further details of the observation programme and the star observing strategy).

By means of the real-time attitude determination, the expected star position in the field of view needed to pilot the image dissector tube was computed as a function of time. With this information, the star observation pattern was converted into a series of coil current pairs, which commanded the instantaneous field of view of the image dissector tube to the star images to be observed. The resulting image dissector tube counts per sampling period were inserted into the satellite telemetry as a continuous data stream. The corresponding observation frame characteristics were inserted into the telemetry by the central on-board software as data packets.

In addition to providing the on-board attitude reference, the star mapper performed astrometric and photometric measurements as part of the Tycho experiment. The light passing through the star mapper grid was measured with two photomultiplier tubes in two different colours, the B_T and V_T channels. The photomultiplier counts per sampling period, after data compression, were also inserted into the satellite telemetry as a continuous data stream.

1.6. Operational Concept

The complexity of on-board processing, and the intensive ground segment involvement, required that the system design was based on a clear operational concept.

Hipparcos was designed as a geostationary satellite with permanent single station ground contact, run to the maximum extent from the ground. On-board processing was intended only if ground processing was prohibitive due to excessive uplink rates (e.g. the implementation of the star observing strategy), or was not feasible due to the telemetry or telecommand turnaround time (e.g. attitude determination and control, image dissector tube piloting). On-board scientific data reduction was not accepted, in order to avoid systematic errors imposed by the associated modelling. The ground segment was designed to monitor satellite health and to initiate corrective actions in case of failure. Only if a failure required a fast reaction to avoid permanent damage to the satellite was an automatic back-up mode provided.

Normal operation was to be performed by means of on-board computers and software. Re-configuration and configuration status monitoring would be performed on a higher, independent level. Automatic back-up modes would override normal operation and configuration. Direct ground commands would override any automatic back-up mode.

During transfer and drift orbit, the satellite would be spinning, and its survival would depend on the proper function of the active nutation damping. A malfunction resulting in excessive nutation would be detected on-board by an accelerometer. It would trigger an automatic switch-over to a completely redundant control and actuation system.

In the intended geostationary phase, when the solar arrays were deployed and the satellite was three-axis controlled, the satellite would be sensitive to attitude errors. At excessively large solar aspect angles, partial shadowing could damage the solar cells and direct sunlight could blind the payload. In sunlight, an attitude error would be detected by a special attitude anomaly detector. An automatic sun acquisition would be triggered by independent back-up hardware. In eclipse, an attitude error would be detected by monitoring the thruster actuations. An anomaly would trigger an automatic spin-up to increase the gyroscopic stiffness. This would keep the satellite in a safe attitude sufficiently long for the ground segment to detect the failure and initiate recovery actions.

Permanent electrical power supply would be essential for the survival of the satellite. Anomalies would be detected through main-bus undervoltage and battery-cell under-voltage, and these would trigger an automatic shedding of non-essential loads.

1.7. Satellite Mechanical and Electrical Design

The satellite consisted of two major hardware elements, namely the spacecraft and the payload. These two hardware elements, together with the on-board software made up the satellite system. As the satellite exploded view shows (Figure 1.6), there was a spacecraft module providing: structural support for its subsystems and for the payload via the interface structure; electrical power supply by solar arrays and batteries; telecommunication and data handling; and the attitude and orbit control required to place the satellite on station and then execute the scanning law. Another spacecraft element was the apogee boost motor, which was designed to inject the satellite from transfer-orbit apogee into near-synchronous orbit. Finally, there was the shade structure needed to provide a stable thermal environment for the payload. The Hipparcos launch and on-station configurations are shown in Figure 1.7.

The electrical subsystems are listed in Table 1.1. The primary power supply was a regulated 50 V DC power bus. At subsystem level (data handling, attitude and orbit control, and payload), there were DC/AC inverters supplying the units with square wave 50 V AC power. The communication between subsystems was through the ESA-standard on-board data handling bus.

The electrical power subsystem supplied the primary electrical power, generated by the solar generator, to the payload and the spacecraft subsystems. Power distribution was through a 50 V DC mains regulated bus and AC secondary power buses. Two rechargeable nickel-cadmium batteries, each with the capacity of 10 Ah, provided continuous power supply during launch and eclipse periods.

The solar generator provided electrical power by use of solar cells arranged on three identical solar panels. The subsystem generated electrical power in transfer orbit when the solar arrays were folded against the satellite body, as well as in operational orbit when the panels were deployed. When deployed, the three panels together provided

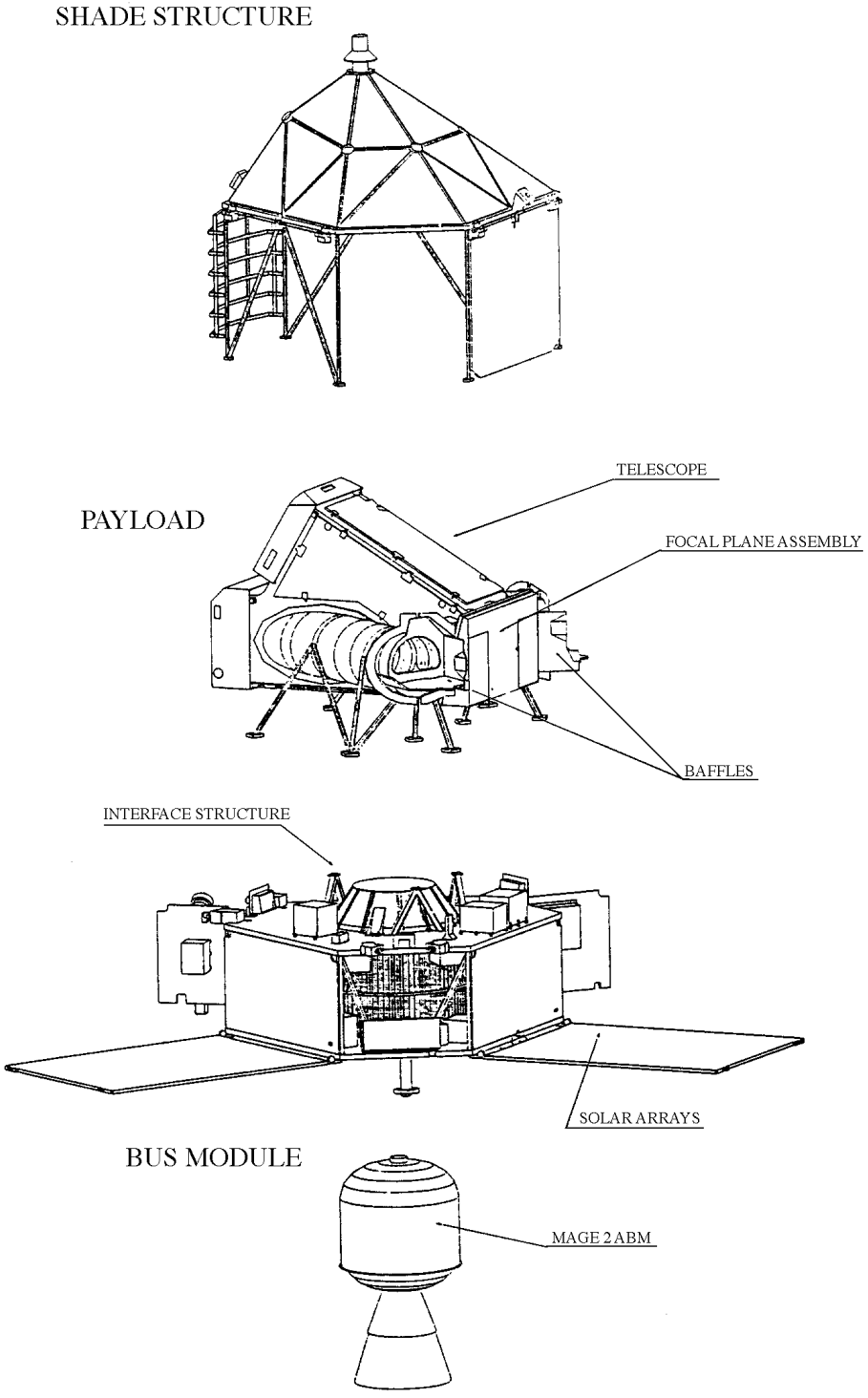

Figure 1.6. *Exploded view of the satellite, illustrating the location of the two fields of view within the payload.*

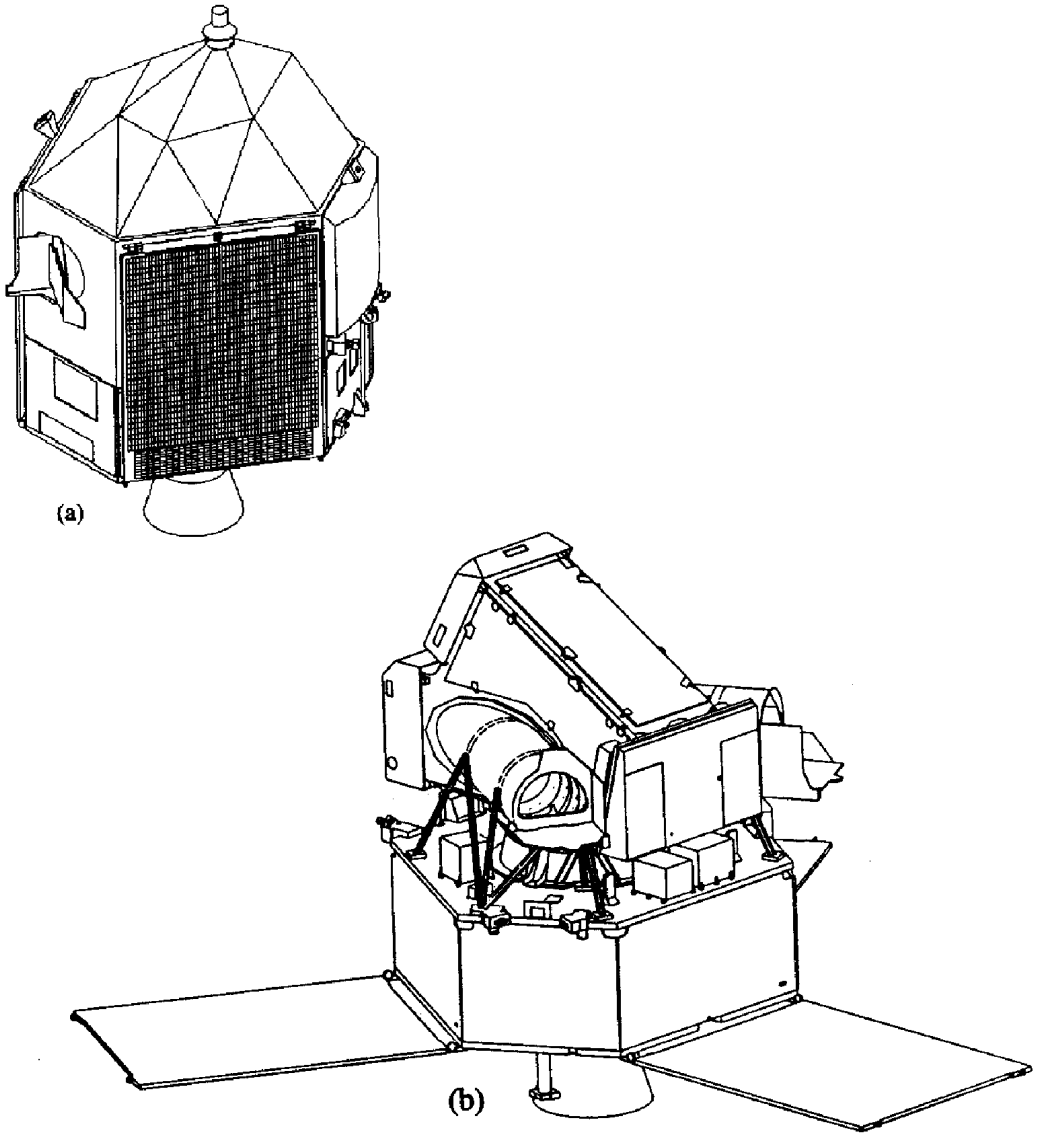

Figure 1.7. *(a) Satellite launch configuration with the solar arrays stowed, and (b) on-station configuration with the solar arrays deployed (and with the shade structure removed for illustration purposes).*

some 350 W of power to the on-board systems. The adopted scanning law meant that the solar panels were at a constant inclination to the Sun throughout routine operations.

Some of the main characteristics of the satellite and its operational environment are listed in Table 1.2. The mass budget for the satellite at launch, rounded to the nearest kilogram, is given in Table 1.3. The power budget is given in Table 1.4 for the pre-operational phase (i.e. in transfer and near synchronous orbit, when the satellite was spinning, the solar arrays were stowed and the payload and on-board computer were off), and for the operational phase (i.e. when the satellite was spinning, the solar arrays were deployed and at a sun aspect angle of 43°).

Table 1.1. Electrical subsystems and acronyms.

Subsystem Description	Acronym
Telecommunication subsystem	TCMS
Data handling subsystem	DHSS
Solar generation subsystem	SGSS
Electrical power subsystem	EPSS
Spacecraft thermal control subsystem	STCS
Attitude and orbit control subsystem	AOCS
Reaction control assembly	RCA
Detection subsystem	DTSS
Payload service electronics units	SEU

Table 1.2. Main satellite characteristics.

Launch mass	1140 kg
Power requirements	295 W (nominal)
Uplink data rate	2 kbits s^{-1}
Downlink data rate	24 kbits s^{-1}
Satellite orbit	Geostationary transfer (Geostationary planned)
Inclination to sun	43°
Spin rate	11.25 rev per day (168.75 arcsec s^{-1})

Table 1.3. Satellite mass budget.

Element	Mass (kg)
Spacecraft	400
Payload	210
Apogee boost motor propellant	463
Hydrazine (expelled after station acquisition)	32
Cold gas (nitrogen)	10
Balancing mass	25
Total launch mass	1140

Table 1.4. Satellite power budget for the pre-operational and operational periods.

System	Pre-operational Period (W)	Operational Period (W)
Electrical power subsystem	22	22
Telecommunication subsystem	31	31
Data handling subsystem	21	45
Attitude and orbit control subsystem	31	80
Spacecraft thermal control	10	3
Payload thermal control	–	64
Payload	–	25
Total	115	270
Solar generation power	155	368

1.8. Ground Segment Overview

Ground segment activities were controlled throughout the mission from the European Space Operations Centre (ESOC) whose role throughout the mission was to ensure that the maximum science data was collected with the best quality possible. This implied that not only the safety of the satellite was ensured, but also its efficiency was kept as high as possible at all times. This was achieved by setting up a mission control team several years before launch to prepare it and to operate the mission after launch. To do this, the team organised a ground segment which comprised all the facilities needed to control the satellite and collect the science data.

The operations team throughout the routine phase comprised some twenty persons. While the functions of the control team were numerous, they could be separated into the following three major areas:

(a) the first group, the spacecraft control team, dealt with the monitoring and control of the satellite, the creation of the mission plan, the command generation, the management of spacecraft parameters and commands (ground-resident satellite data base), the spacecraft performance evaluation, and the on-board software updates;

(b) the second group, the flight dynamics team, dealt mainly with the real-time attitude monitoring and correction of the spacecraft, the programme star file generation, mission plan preparation, the payload performance monitoring, the payload calibrations, and the Hipparcos Input Catalogue maintenance;

(c) the third group, the software support team, was responsible for maintaining the software which processed telemetry and telecommanding in real-time. In addition they performed the data archiving and produced the final tapes which were sent to the Hipparcos data reduction consortia for subsequent processing.

In addition to the above, ESOC infrastructure support guaranteed appropriate hardware availability, the scheduling of ground station coverage, the link configurations to the various ground stations and computers, satellite ranging support, orbit determination and other facilities common to all ESOC controlled satellites.

The Hipparcos ground segment was originally intended to comprise only a single ground station at Odenwald, combined with the operations control centre at ESOC. With the non-nominal 10.66-hour orbit, a single ground station would have provided only limited operational coverage, insufficient to allow the development of an interconnected observational network critical to the data reduction concept. Within a few months of launch, additional ground stations were brought into the network, so that the final operational network ultimately comprised three major elements: ground stations located in Odenwald (Germany), Perth (Australia), Kourou (French Guyana) and Goldstone (USA); the operations control centre at the European Space Operations Centre in Darmstadt, Germany; and a communications system interconnecting these sites.

During the mission, the spacecraft was controlled from the following control rooms based at ESOC: (i) the operations control centre had the overall responsibility for all satellite and mission control activities; (ii) the main control room was only used during

critical mission control phases or emergency operations; (iii) all routine operations were controlled from the Hipparcos dedicated control room. This room was equipped with three workstations connected to the Hipparcos dedicated computer system; (iv) the flight dynamics room was used during critical mission phases and important manoeuvres, with the routine flight dynamics attitude and payload functions transferred to the Hipparcos dedicated control room to ease the operational interface between the control teams; and (v) the ground control room established the connections between the relevant ground stations and the operations control centre as well as the data line connections between the computer systems.

The main control room was used during the launch and early orbit phase of the mission. All operations were performed using the allocated general-purpose interactive workstations which interfaced with the data processing facilities and data files of the Hipparcos dedicated control system computer. Ranging operations were initiated from the multi-satellite support system. Each workstation was equipped with three displays for alphanumeric and graphical presentation of telemetry data in real-time or retrieval mode. Hardcopy devices allowed instant record of the displays. The operations control center had a number of intercom voice loops which allowed two-way voice communications between all teams in the operations control center, the ground stations and the launch range.

During the routine phase of the mission, the dedicated control room was used for all monitoring and control functions. The room was equipped with three workstations and had in addition terminals connected to the off-line computer. Hardcopy devices were attached to each workstation. Voice loop and telephone communications facilities were provided. During critical or contingency phases additional workstations were connected on-line in the main control room.

The flight dynamics control room was equipped with terminals to both the on-line and the off-line Hipparcos computers as well as to the multi-satellite support system computers for use in the launch and early operations phase. Hardcopy facilities were available for printing information from the computer displays. Voice contact between the main control room and/or dedicated control room was possible by means of the intercom facility.

The Hipparcos operational software consisted of two separated systems: (i) the on-line software, providing support to all activities related to the near real-time satellite control operations, and (ii) the off-line software, providing support to all non real-time activities.

The on-line software was resident on a VAX 785 machine, with a VAX 785 as back-up (one of the VAX 785 computers was replaced by a more powerful VAX 8650 machine in January 1990). In addition, a VAX 4090 workstation was installed in early 1993 to deal with the large increase in software demands precipitated by the satellite's gyro failures. The off-line software (referred to as the multiple virtual system, or MVS) was run on a Comparex 8/96 mainframe computer, the two computers being interconnected by a high-speed data link. This allowed the use of both machines during some on-line activities, such as the programme star file production, and payload calibration and monitoring. Additional off-line processing was supplied on an IBM-PC PS/2 for use in performing real-time attitude determination.

The on-line software supported the following tasks: the telemetry processing chain, the telecommanding chain, real-time operator interface, maintenance of operational data bases, telemetry filing and archiving, report generation, and ranging support. In

addition it also supported on-board computer and control law electronics monitoring and updating real-time attitude monitoring, ground real-time attitude determination, payload performance monitoring, real-time payload calibration, and link control and monitoring.

In addition to the Hipparcos specific software, a number of general software facilities were implemented on the on-line software system. This general software was called the spacecraft control and operating system, or SCOS, and provided standard telemetry processing, workstation displays, reading telemetry data from history files, and data base editing facilities.

The off-line software system concentrated on the following tasks: off-line telecommand preparation, on-board software maintenance, spacecraft performance evaluation system, mission planning support, programme star file support, Hipparcos Input Catalogue maintenance, payload calibrations and monitoring, calibration support and analysis, data reduction consortia tape production, and star pattern matching.

In addition, orbit determination was performed on the multi-satellite support system.